

Exciton dispersion in *para*-quaterphenyl: Significant molecular interactions beyond Coulomb coupling

Cite as: AIP Advances 11, 095313 (2021); <https://doi.org/10.1063/5.0058657>

Submitted: 29 June 2021 • Accepted: 02 September 2021 • Published Online: 17 September 2021

 Lukas Graf, Yulia Krupskaya, Bernd Büchner, et al.



View Online



Export Citation



CrossMark

ARTICLES YOU MAY BE INTERESTED IN

[Modeling nonlocal electron-phonon coupling in organic crystals using interpolative maps: The spectroscopy of crystalline pentacene and 7,8,15,16-tetraazaterrylene](#)

The Journal of Chemical Physics **153**, 124113 (2020); <https://doi.org/10.1063/5.0021731>

[Addressing the Frenkel and charge transfer character of exciton states with a model Hamiltonian based on dimer calculations: Application to large aggregates of perylene bisimide](#)

The Journal of Chemical Physics **154**, 124101 (2021); <https://doi.org/10.1063/5.0045913>

[Two-dimensional electronic-vibrational spectroscopy: Exploring the interplay of electrons and nuclei in excited state molecular dynamics](#)

The Journal of Chemical Physics **155**, 020901 (2021); <https://doi.org/10.1063/5.0053042>

Call For Papers!

AIP Advances

SPECIAL TOPIC: Advances in

Low Dimensional and 2D Materials



Exciton dispersion in *para*-quaterphenyl: Significant molecular interactions beyond Coulomb coupling

Cite as: AIP Advances 11, 095313 (2021); doi: 10.1063/5.0058657

Submitted: 29 June 2021 • Accepted: 2 September 2021 •

Published Online: 17 September 2021



View Online



Export Citation



CrossMark

Lukas Graf,  Yulia Krupskaya, Bernd Büchner, and Martin Knupfer^{a)} 

AFFILIATIONS

IFW Dresden, Helmholtz Str. 20, D-01069 Dresden, Germany

^{a)} Author to whom correspondence should be addressed: m.knupfer@ifw-dresden.de

ABSTRACT

We have experimentally determined the momentum dependence of the electronic excitation spectra of *para*-quaterphenyl single crystals. The parallel arrangement of *para*-quaterphenyl molecules results in a strong Coulomb coupling of the molecular excitons. Such crystals have been considered to be a very good realization of the Frenkel exciton model, including the formation of H-type aggregates. Our data reveal an unexpected exciton dispersion of the upper Davydov component, which cannot be rationalized in terms of inter-molecular Coulomb coupling of the excitons. A significant reduction of the nearest neighbor coupling due to additional charge-transfer processes is able to provide an explanation of the data. Furthermore, the spectral onset of the excitation spectrum, which represents a heavy exciton resulting from exciton–phonon coupling, also shows a clear dispersion, which had been unknown so far. Finally, an optically forbidden excitation about 1 eV above the excitation onset is observed.

© 2021 Author(s). All article content, except where otherwise noted, is licensed under a Creative Commons Attribution (CC BY) license (<http://creativecommons.org/licenses/by/4.0/>). <https://doi.org/10.1063/5.0058657>

I. INTRODUCTION

Organic semiconductor research and applications have developed in previous years, and applications such as light-emitting diodes and organic photovoltaic cells have entered the market already.^{1–6} The properties of such devices strongly depend on the photophysical behavior of the used organic semiconducting materials. Therefore, there is particular interest to deeply understand the character of electronic excitations in organic semiconductors, which then allows us to optimize, model, and predict new materials' properties as well as device performances.

In the solid-state, inter-molecular interactions, which strongly depend on the molecular packing, play an important role in the determination of the photophysical behavior as well as of the energy transport. The impact of molecular packing on basic optical properties, such as absorption and photoluminescence, was originally worked out for arrangements dominated by Coulombic intermolecular interactions,^{7,8} eventually leading to the classification of J- and H-aggregates and the description of the exciton band structure based on these interactions. Later, it became clear that a detailed treatment of the coupling of the molecular (Frenkel) excitons to

phonons or vibrations and the consideration of inter-molecular charge-transfer processes are required to obtain a good description and understanding of the photophysical behavior of a number of organic materials.^{9–20} One of the important results of these studies is an advanced theoretical picture of the exciton band structure in the respective materials. On the experimental side, however, only in a few cases, this exciton band structure has been determined directly, despite its importance for a full understanding of the materials' photophysics and for a verification of the models proposed.^{21–26}

In this paper, we present an experimental determination of the exciton dispersion in *para*-quaterphenyl single crystals measured using electron energy-loss spectroscopy (EELS). *para*-quaterphenyl is a representative of conjugated oligomer herringbone aggregates, which are characterized by quite strong exciton coupling via the Coulomb interaction of the excitation dipole moment of adjacent molecules. The strong exciton coupling is a result of the closely packed molecules in the crystal structure in combination with a relatively weak dielectric screening in such molecular crystals. In contradiction to previous calculations based on this dipole–dipole interaction,²⁷ our data signal an unexpected and quite complex

exciton dispersion with a shallow minimum in the Brillouin zone. Further contributions to the exciton coupling based on charge-transfer processes might cause this behavior. Our data additionally reveal the dispersion of the spectral onset, which provides first insight into the momentum dependence of a heavy exciton at this energy. In addition, we observe the appearance of an optically forbidden excitation at somewhat higher energies.

II. EXPERIMENTAL AND CRYSTAL CHARACTERIZATION

para-quaterphenyl (p-4P) single crystals were grown by physical vapor transport²⁸ in a furnace consisting of a quartz tube with a resistive heater used to establish a temperature gradient. Pure argon gas was chosen as the carrier gas. Quaterphenyl powder (purchased from TCI) was placed in the hotter end of the furnace, and the sublimed molecules were transported to the colder end, where the crystal growth took place. The resulting p-4P single crystals were carefully selected with the help of a microscope and placed on standard transmission electron microscopy grids. For the subsequent EELS studies, a crystal thickness of about 100 nm is required, and the lateral dimension of the crystals was about 2–5 mm.

All electron diffraction data and electronic excitation spectra have been obtained using a purpose-built electron energy loss spectrometer for EELS in transmission.^{29,30} EELS is well suited to study electronic excitations as a function of momentum transfer.^{31–33} All data have been taken at a sample temperature of 20 K, which substantially reduces sample damage by the electron beam and thermal broadening. The energy and momentum resolution have been 85 meV and 0.035 \AA^{-1} , respectively. The EELS signal, which is proportional to the loss function $\text{Im}[-1/\epsilon(\mathbf{q}, \omega)]$, was determined for various momentum transfers, \mathbf{q} , parallel to directions of the corresponding reciprocal lattice vectors.

Electron diffraction was used to prove the successful crystal growth and to select the direction of the momentum transfer vector in the reciprocal space. These diffraction data perfectly agree with the low temperature crystal structure of p-4P,³⁴ which is triclinic (space group P1, $Z = 4$) with lattice parameters $a = 9.74 \text{ \AA}$, $b = 9.74 \text{ \AA}$, $c = 17.70 \text{ \AA}$, $\alpha = 85.40^\circ$, $\beta = 94.60^\circ$, and $\gamma = 110.11^\circ$.³⁴ The corresponding data are shown in Fig. 1.

III. RESULTS AND DISCUSSION

para-quaterphenyl undergoes an order-to-disorder transition in a quite broad temperature range around 230 K,^{35–41} where the molecules become non-planar at lower temperatures. Below this transition, the average rotation angle from the mean planar high-temperature configuration is 5.8° for the end phenyl rings and 11.3° for the inner rings.³⁴ However, the mutual arrangement of the molecules and their distances remain almost unchanged, and the long molecular axes remain parallel, i.e., the structural modification results essentially from the rotations of the phenyl rings about the long molecular axes. Therefore, the low temperature crystal structure can also be described by a pseudomonoclinic supercell with lattice constants: $\tilde{a} = 15.97 \text{ \AA}$, $\tilde{b} = 11.16 \text{ \AA}$, $\tilde{c} = 17.70 \text{ \AA}$, and $\tilde{\beta} = 95.61^\circ$,³⁴ where the \tilde{a} and \tilde{b} lattice parameters are doubled in comparison to the high temperature phase.^{34,42,43} Moreover, the phenyl ring rotation angles are quite

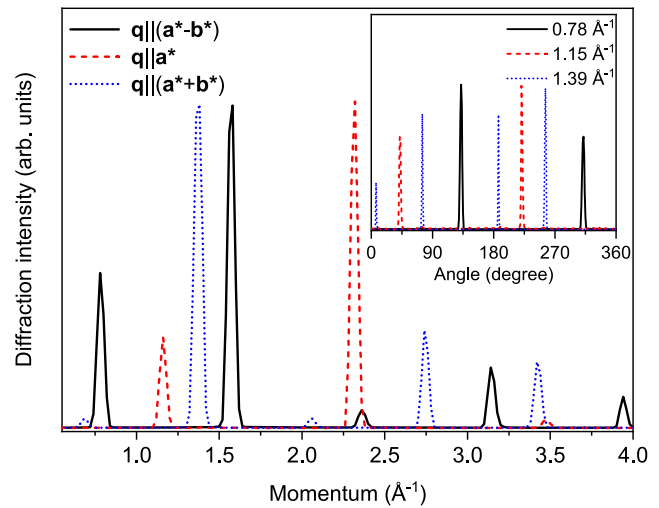


FIG. 1. Representative electron diffraction profiles of a p-4P single crystal at 20 K. The data show measurements along the fundamental reciprocal lattice directions ($\mathbf{a}^* - \mathbf{b}^*$), \mathbf{a}^* , and $(\mathbf{a}^* + \mathbf{b}^*)$ of the low temperature, triclinic crystal structure.³⁴ Inset: electron diffraction profiles measured for a fixed momentum transfer value, q , in the \mathbf{a}^* , \mathbf{b}^* -plane. The observed relative angles agree very well with the low temperature crystal structure.³⁴

small and thus have a minor effect on the molecular orbitals. Consequently, it is reasonable to expect that the electronic excitations also hardly change at this order-to-disorder transition as is indicated by optical data of p-4P crystals around the absorption onset⁴⁴ and those from the close relative *para*-hexaphenyl in thin film form.⁴⁵

It is already known that the electronic excitation spectrum of p-4P crystals is considerably anisotropic.^{27,46,47} Figure 2

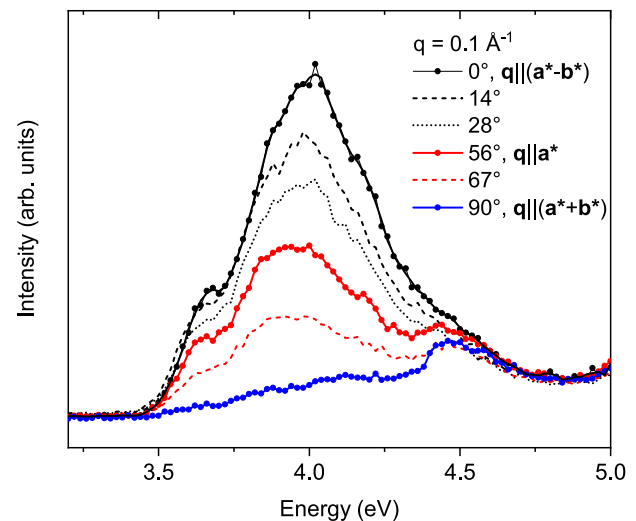


FIG. 2. Electronic excitation spectra of p-4P crystals for a small momentum transfer of $q = 0.1 \text{ \AA}^{-1}$, which corresponds to the optical limit. The data are taken with different angles of the momentum vector with respect to the $(\mathbf{a}^* - \mathbf{b}^*)$ reciprocal direction, and they document the strong anisotropy (polarization dependence) of the lowest exciton feature.

demonstrates this strong anisotropy. Note that our notation for the reciprocal axes corresponds to the triclinic (low temperature) unit cell. Furthermore, our momentum is always oriented along the reciprocal direction, which is not parallel to the principle crystal axes due to the low symmetry of the unit cell. However, our data with a momentum along the reciprocal direction ($\mathbf{a}^* - \mathbf{b}^*$) can be reasonably well compared to optical data with a light polarization parallel to the (monoclinic) $\tilde{\mathbf{a}}$ crystal axis of the high temperature phase as these two directions enclose an angle of just 14° .⁴² Figure 2 also reveals that the shape of the spectra is quite broad and of some complexity. If we ignore the intra-molecular ring rotations that occur at the order-to-disorder transition, the low temperature structure can also be described by a unit cell containing two p-4P molecules. Their long axis is parallel to each other and encloses an angle with the lattice \mathbf{c} axis of a few degrees.^{34,42,43} In p-4P molecules, the molecular dipole moment of the first excited state is aligned exactly parallel to the long molecular axis,²⁷ and a sizable Coulomb interaction of the excitation dipole moment of adjacent molecules is expected. According to Davydov,⁸ a given molecular electronic level splits up in crystals due to this interaction in as many components as there are translationally inequivalent molecules in the unit cell. As a consequence, two exciton levels (Davydov components) are formed in p-4P crystals. Furthermore, the crystal states of the Davydov components along the symmetry axes in reciprocal space are the symmetric and anti-symmetric combinations of the wave functions of the corresponding sublattices. In p-4P, the oscillator strength of the upper Davydov component is proportional to the sum of the individual molecular transition moments, while that of the lower Davydov component is proportional to the corresponding difference. Finally, as a consequence of the orientation of the molecules in the p-4P crystal, the upper Davydov excitation is polarized within the $\tilde{\mathbf{a}}, \tilde{\mathbf{c}}$ -plane of the monoclinic, high temperature phase, while lower Davydov excitation is polarized along the monoclinic $\tilde{\mathbf{b}}$ axis. Translated into the triclinic low temperature notation, our measurements for a momentum direction, \mathbf{q} , parallel to the $(\mathbf{a}^* - \mathbf{b}^*)$ direction represent the upper Davydov component, which is strong in intensity. Those for \mathbf{q} parallel to $(\mathbf{a}^* + \mathbf{b}^*)$, in turn, represent the lower Davydov component, with negligible intensity. All this is well represented by our EELS data, as shown in Fig. 2 as a function of the direction of the momentum vector in the $\mathbf{a}^*, \mathbf{b}^*$ -plane. We associate the strong feature at about 4 eV to the excitation of the upper Davydov component, which agrees well with its polarization dependence and with calculations of the electronic excitations.^{27,46,47} The lower Davydov component is expected to carry no spectral weight since the molecular dipole moments cancel.²⁷

Moreover, the upper Davydov component is very broad in energy and additional excitation features at about 3.68 and 4.5 eV are observed in Fig. 2. These observations are not explained by the picture outlined above. It is well known that already the optical absorption spectrum of p-4P molecules in solution is very broad in energy.^{27,43,48} This has been assigned to the coupling of the electronic excitation to torsional ring motions in the molecules,^{49,50} which is also present in the crystal. In addition, previous theoretical studies using a multimode exciton-phonon Hamiltonian have pointed out that there can be substantial exciton-phonon coupling in conjugated oligomer herringbone aggregates.^{12,51-53} In particular, there can be inter-molecular Herzberg-Teller coupling between the lower Davydov component and the upper Davydov component,

which is provided by asymmetric phonons. Then, heavily dressed excitons can exist at an energy of the lower Davydov component plus the related phonon energy, whereas the absorption spectral weight and the polarization dependence are borrowed from the upper Davydov component. In other words, the appearance of heavy excitons in the spectra for momentum vectors (or polarization) parallel to $(\mathbf{a}^* - \mathbf{b}^*)$ can be explained to be of false origin arising from such a coupling.^{12,51-53}

These heavy exciton states can explain the low-energy region and the fine structure of the optical absorption spectrum starting from the absorption onset up to the main absorption maximum. Accordingly, we assign the lowest excitation features at about 3.38 eV as seen in Fig. 2 for the $(\mathbf{a}^* - \mathbf{b}^*)$ reciprocal direction to such a heavy exciton. The origin of the additional excitation feature at about 4.5 eV, which is most prominently seen in the spectrum for momenta close to the $(\mathbf{a}^* + \mathbf{b}^*)$ reciprocal direction, most likely is not due to exciton-phonon coupling, since its energy is too far above the excitation maximum. Interestingly, this feature had already been reported in crystal absorption data at room temperature.²⁷ In view of calculations of the dielectric tensor of p-4P crystals, a symmetry forbidden excitation with B_{3g} symmetry might be located around 4.5 eV, and it may become visible due to the admixture of vibrations. We will further discuss this issue below in the context of the momentum dependent EELS spectra.

We now turn to the momentum dependence of the electronic excitation spectra, i.e., the exciton dispersion. We restrict ourselves to the reciprocal direction in which the excitation intensity is strongest and clearly visible, i.e., for a momentum vector parallel to the $(\mathbf{a}^* - \mathbf{b}^*)$ direction. The corresponding data are depicted in Fig. 3 and they demonstrate a quite complex momentum behavior of the excitons. Most obviously, the main feature located at about 4 eV at low momentum transfer clearly moves to lower energies upon increasing momentum values up to about 0.5 \AA^{-1} , and then there is a small upshift resulting in a shallow minimum. In addition, the leading edge of the excitation spectra or their onset also shifts

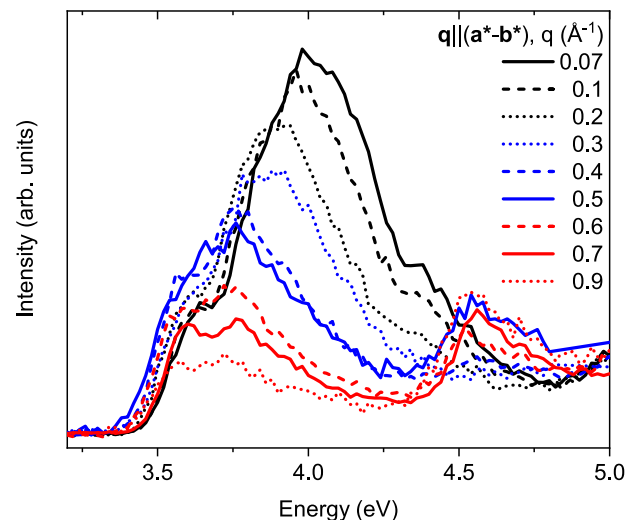


FIG. 3. Momentum dependent electronic excitation spectra of p-4P crystals for momentum vectors parallel to the $(\mathbf{a}^* - \mathbf{b}^*)$ reciprocal direction.

to lower energies with growing momentum and reaches its lowest position also at about 0.5 \AA^{-1} before it also increases in energy for higher momenta. The fact that there is a clear relation of energy and momentum shows that the momentum, q , can be used to represent the exciton states, i.e., these excitons are delocalized and the associated energy transfer occurs in a wavelike or coherent manner. We note that the coupling of the electronic excitations to torsional ring motions in the molecules, which explains the spectral width of the upper Davydov component,^{49,50} does not destroy exciton coherence in p-4P. Finally, there is a new excitation feature arising with increasing momentum transfer values, which is located at about 4.5 eV and which does not change in energy.

In order to quantify the dispersion of the excitation features, we have analyzed the energy–momentum behavior of the spectra as follows. The leading edge of the spectra has been determined via the maximum of their first derivative as a function of energy. We assume that this leading edge position is representative of the energy of the heavy exciton but is downshifted by about 0.1 eV. The maximum of the main feature assigned to the upper Davydov component can be read off the data directly with an accuracy of about 100 meV. The results of this analysis are shown in Fig. 4. Clearly, both excitations show negative dispersion up to about 0.5 \AA^{-1} but then increase in energy for higher momenta.

The parallel arrangement of the molecules in p-4P crystals and thus also of the transition dipole moments results in an H-type interaction, and in the optical limit, excitations can only occur into the

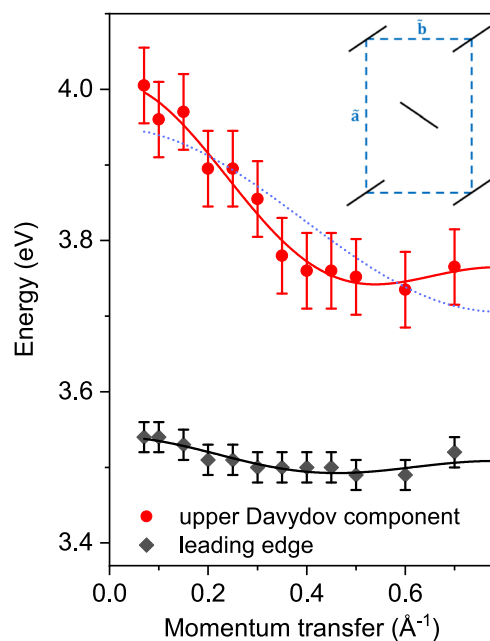


FIG. 4. Energy of the upper Davydov component and the leading edge (see Fig. 3) as a function of momentum transfer (symbols). The solid lines represent the fits [Eq. (2)], as described in the text. The dotted line represents the description of the upper Davydov component based upon nearest neighbor coupling only [Eq. (1)] in order to illustrate the insufficient description of the dispersion. The upper right inset shows a schematic view on the molecular arrangement in the crystal viewed along the monoclinic \bar{c} direction (for details, see Refs. 34, 42, and 43).

upper Davydov component.^{8,54} Furthermore, although the unit cell contains more than one molecule, this parallel arrangement makes the inter-molecular exciton coupling invariant to translations to the nearest neighbors. Thus, the exciton dispersion can be discussed in a simple lattice containing a single molecule per unit cell.⁵⁴ In the simplest approximation, exciton coupling would be restricted to Coulomb coupling of the excited state charge distributions of nearest neighbors, which we call J_{Coul} . Often, J_{Coul} is derived using the point dipole approximation. The resulting exciton band structure for the upper Davydov component would be given by a cosine function ($J_{Coul} = J_0$),

$$E(q) = E_0 + 4 J_0 \cos\left(\frac{q}{2} \bar{a}\right), \quad (1)$$

where \bar{a} denotes the molecular distance along the monoclinic \bar{a} axis ($\bar{a} = 7.985 \text{ \AA}$ at low temperature³⁴) and q is the measured momentum value, as shown in Fig. 4. Clearly, the observed exciton dispersion of the upper Davydov component does not follow this simple expectation. Following the considerations and calculations for oligothiophenes, we therefore have taken next-nearest neighbor, J_1 , interactions into account, which gives rise to the following exciton dispersion:⁵⁴

$$E(q) = E_0 + 4 J_0 \cos\left(\frac{q}{2} \bar{a}\right) + 2 J_1 \cos(q \bar{a}). \quad (2)$$

Using this equation, we can very well describe the measured dispersion of the (H-type) upper Davydov component. This is demonstrated in Fig. 4, where the solid line through the data is a result of a fit of the data with this equation. The resulting parameters are $E_0 = 3.83 \text{ eV}$, $J_0 = 30.6 \text{ meV}$, and $J_1 = 27.8 \text{ meV}$. This represents a quite unexpected result. Previous calculations of the exciton dispersion in p-4P based on macroscopic dielectric theory predicted an exciton bandwidth $W = 8J_0$ of about 400 meV,²⁷ significantly larger than our result of $W = 244 \text{ meV}$. In addition, a dispersion relation $E(q) \propto \cos\left(\frac{q}{2} \bar{a}\right)$ has been predicted, which is in contradiction to the experiments. Moreover, the obtained ratio of the coupling parameters, J_1/J_0 , of about 0.9 is much larger than one would expect based on the point dipole approximation, where this ratio would be given by the corresponding molecular distances in the lattice $(r_0/r_1)^3 = 0.226$. We therefore conclude that a description of the upper Davydov exciton in p-4P based on Coulomb coupling is insufficient. There must be an additional contribution, which changes, in particular, J_0 substantially.

For a number of organic semiconductors, it has been pointed out in the past that there can be additional, quite large exciton coupling via charge-transfer (CT) processes, which arises from the wave function overlap between neighboring molecules.^{9–20} These CT processes are governed by the electron and hole transfer integrals, t_e and t_h , respectively, and they diminish exponentially with distance. Therefore, we consider these CT processes to contribute to J_0 only. Furthermore, in a perturbative limit, when the CT excitations are energetically well above the intra-molecular Frankel ones, the two coupling sources, J_{Coul} and J_{CT} , are additive: $J_0 = J_{Coul} + J_{CT}$.¹⁹ Importantly, the sign of J_{CT} depends on the relative signs of t_e and t_h , and it can thus be negative and in the case of p-4P reduce the total nearest neighbor coupling J_0 . To conclude at this point, our results indicate that the dispersion of the upper Davydov exciton is determined by an interesting interplay between Coulomb and charge-transfer

coupling, which results in the formation of a shallow dispersion minimum at finite momentum in the Brillouin zone as depicted in Fig. 4. We note that the coupling between the excitons and several (low and high energy) vibrational modes may have significant impact on the exciton behavior.²⁰ For instance, it has been shown that the consideration of coupling to low and high energy modes is necessary to model the polarized absorption and photoluminescence of oligothiophenes and oligophenylene crystals.^{20,54,55} It is at least conceivable that the exciton dispersion is also altered by this multi-vibronic coupling in conjunction with sizable Coulomb and charge-transfer exciton transfer.

The leading edge position, which may represent the “heavy exciton,”⁵¹ also shows a negative dispersion up to about 0.4–0.5 eV but with a much smaller bandwidth of about 50 meV, as expected for a heavy exciton.⁵¹ For higher momentum transfer values, the energy increases and reaches about the value of zero momentum again. In other words, our data reveal the band structure of this exciton, which has not been discussed in the literature so far. We have also used Eq. (2) to model the dispersion relation of the low energy, heavy exciton, and we have obtained the following parameter set: $E_0 = 3.509$ eV, $J_0 = 4$ meV, and $J_1 = 7.5$ meV. These parameters reflect the substantially smaller exciton bandwidth and, intriguingly, indicate that next nearest coupling, J_1 , is larger than nearest neighbor coupling, J_0 . Detailed theoretical modeling, which is far beyond the scope of this paper, is required to more deeply understand this behavior.

In general, electron energy-loss spectroscopy can also be applied to probe the multipole character of local electronic excitation, i.e., those that occur on e.g., one molecule only with negligible impact from the neighbors.^{31,56–68} In particular, non-dipole allowed excitations show up in the spectra at higher momentum transfer, which allows, for instance, to determine their energy in contrast to optical absorption experiments. The intensity increase of such non-dipole allowed excitations as a function of momentum transfer depends on the spatial extension of the excitation (i.e., on the average electron–hole distance). The excitation at about 4.5 eV (see Fig. 3) becomes visible around 0.4 \AA^{-1} , where its intensity is large enough as compared to the background and satellite structure related to the lower energy excitations. The following significant intensity rise and the virtually momentum independent energy strongly support the interpretation as a non-dipole allowed or optically forbidden molecular excitation.^{31,56–68} From the continuous intensity rise up to 0.9 \AA^{-1} , we can conclude that its spatial extension is not larger than about a few \AA , which is in good agreement to the size of a benzene ring.

IV. CONCLUSIONS

We have analyzed the exciton dispersion in *para*-quaterphenyl single crystals using electron energy-loss spectroscopy. The molecular excitation dipole of the lowest electronic excitation in *para*-quaterphenyl molecules is oriented parallel to the long molecular axis, and the molecules are arranged in a parallel or side-by-side manner in the crystal structure. As a consequence, there is quite substantial Coulomb coupling between the excitation dipoles of adjacent molecules, which should result in so-called H-aggregate formation, leading to a blue shift of the excitation energy with respect to that of individual molecules in the optical limit.¹⁹

In addition, the excitons are expected to show a negative dispersion in this case, i.e., their energy decreases with increasing momentum, which is related to a suppression of the radiative decay rate of the excitons. Although the unit cell of *para*-quaterphenyl crystals contains more than one symmetrically inequivalent molecule, the parallel arrangement renders the inter-molecular coupling invariant to translations to the nearest neighbors, and in very good approximation, the excitons can be described in a simple lattice containing a single molecule per unit cell.⁵⁴ Thus, the exciton dispersion of the upper Davydov component can be discussed in terms of H-aggregate-like excitons.

We show that the upper Davydov component is characterized by a clear dispersion along the $(\mathbf{a}^* - \mathbf{b}^*)$ reciprocal direction, i.e., this exciton moves coherently through the crystal. Moreover, the dispersion is negative at small momenta, which at first glance is expected for H-aggregates.¹⁹ However, the dispersion relation $E(\mathbf{q})$ does not follow the simple expectation for pure molecular (Frenkel) excitons that are Coulomb coupled to their neighbors via the interaction of the excitation dipoles. Our results strongly indicate further contribution to the exciton coupling, which most likely arise from additional charge-transfer (CT) coupling, which is a result of significant wave function overlap between neighboring molecular orbitals. The interference of Coulomb and CT coupling reduces the nearest neighbor interaction in *para*-quaterphenyl crystals. Finally, the spectral width of this upper Davydov feature is relatively broad, which results from a significant coupling between the electronic excitation and the torsional motions within the quaterphenyl molecule. This torsional coupling, however, is not able to destroy the exciton coherence.

The spectral onset, which can be ascribed to a heavy exciton due to exciton–phonon coupling,⁵¹ also shows a dispersion, which has been unknown so far and which is characterized by a much smaller bandwidth. Also in this case, the dispersion does not follow the Coulomb coupling picture, and future theoretical work is necessary to unravel its microscopic origin.

Finally, our data revealed the existence of an optically forbidden excitation, which is about 1 eV above the spectral onset of the excitation spectra. This most likely is a pure, localized molecular excitation that arises from excitations between differently localized molecular orbitals.⁴⁶

ACKNOWLEDGMENTS

We are grateful to M. Naumann, R. Hübel, and F. Thunig for technical assistance. Financial support by the Deutsche Forschungsgemeinschaft within Project Nos. KN393/25, KN393/26, and KR4364/4 is gratefully acknowledged. Financial support by the Open Access Fund of the Leibniz Association and the Deutsche Forschungsgemeinschaft within Project Nos. KN393/25, KN393/26, and KR4364/4 is gratefully acknowledged.

DATA AVAILABILITY

The data that support the findings of this study are available from the corresponding author upon reasonable request.

REFERENCES

- 1 H.-W. Chen, J.-H. Lee, B.-Y. Lin, S. Chen, and S.-T. Wu, *Light: Sci. Appl.* **7**, 17168 (2018).

- ²O. Ostroverkhova, *Handbook of Organic Materials for Electronic and Photonic Devices* (Woodhead Publishing, 2018).
- ³A. Salehi, X. Fu, D. H. Shin, and F. So, *Adv. Funct. Mater.* **29**, 1808803 (2019).
- ⁴Z. Hu, J. Wang, X. Ma, J. Gao, C. Xu, K. Yang, Z. Wang, J. Zhang, and F. Zhang, *Nano Energy* **78**, 105376 (2020).
- ⁵M. Riede, D. Spoltore, and K. Leo, *Adv. Energy Mater.* **11**, 2002653 (2021).
- ⁶G. P. Kini, S. J. Jeon, and D. K. Moon, *Adv. Funct. Mater.* **31**, 2007931 (2021).
- ⁷M. Kasha, H. R. Rawls, and M. Ashraf El-Bayoumi, *Pure Appl. Chem.* **11**, 371 (1965).
- ⁸A. S. Davydov, *Theory of Molecular Excitons* (Plenum Press, New York, 1971).
- ⁹R. E. Merrifield, *J. Chem. Phys.* **34**, 1835 (1961).
- ¹⁰W. L. Pollans and S.-i. Choi, *J. Chem. Phys.* **52**, 3691 (1970).
- ¹¹P. Petelenz, *Phys. Status Solidi B* **78**, 489 (1976).
- ¹²A. Stradomska, W. Kulig, M. Slawik, and P. Petelenz, *J. Chem. Phys.* **134**, 224505 (2011).
- ¹³M. Hoffmann and Z. Soos, *Phys. Rev. B* **66**, 024305 (2002).
- ¹⁴L. Gisslén and R. Scholz, *Phys. Rev. B* **80**, 115309 (2009).
- ¹⁵F. C. Spano and L. Silvestri, *J. Chem. Phys.* **132**, 094704 (2010).
- ¹⁶H. Yamagata, J. Norton, E. Hontz, Y. Olivier, D. Beljonne, J. L. Brédas, R. J. Silbey, and F. C. Spano, *J. Chem. Phys.* **134**, 204703 (2011).
- ¹⁷P. Cudazzo, M. Gatti, A. Rubio, and F. Sottile, *Phys. Rev. B* **88**, 195152 (2013).
- ¹⁸N. J. Hestand, H. Yamagata, B. Xu, D. Sun, Y. Zhong, A. R. Harutyunyan, G. Chen, H.-L. Dai, Y. Rao, and F. C. Spano, *J. Phys. Chem. C* **119**, 22137 (2015).
- ¹⁹N. J. Hestand and F. C. Spano, *Acc. Chem. Res.* **50**, 341 (2017).
- ²⁰N. J. Hestand and F. C. Spano, *Chem. Rev.* **118**, 7069 (2018).
- ²¹M. Knupfer, T. Schwieger, J. Fink, K. Leo, and M. Hoffmann, *Phys. Rev. B* **66**, 035208 (2002).
- ²²R. Schuster, M. Knupfer, and H. Berger, *Phys. Rev. Lett.* **98**, 037402 (2007).
- ²³C. N. Koditwakku, C. A. Burns, A. H. Said, H. Sinn, X. Wang, T. Gog, D. M. Casa, and M. Tuel, *Phys. Rev. B* **77**, 125205 (2008).
- ²⁴F. Roth, R. Schuster, A. König, M. Knupfer, and H. Berger, *J. Chem. Phys.* **136**, 204708 (2012).
- ²⁵F. Roth, P. Cudazzo, B. Mahns, M. Gatti, J. Bauer, S. Hampel, M. Nohr, H. Berger, M. Knupfer, and A. Rubio, *New J. Phys.* **15**, 125024 (2013).
- ²⁶F. Roth, M. Nohr, S. Hampel, and M. Knupfer, *Europhys. Lett.* **112**, 37004 (2015).
- ²⁷S. Blumstengel, F. Meinardi, P. Spearman, A. Borghesi, R. Tubino, and G. Chirico, *J. Chem. Phys.* **117**, 4517 (2002).
- ²⁸R. A. Laudise, C. Kloc, P. G. Simpkins, and T. Siegrist, *J. Cryst. Growth* **187**, 449 (1998).
- ²⁹J. Fink, *Adv. Electron. Electron. Phys.* **75**, 121 (1989).
- ³⁰F. Roth, A. König, J. Fink, B. Büchner, and M. Knupfer, *J. Electron Spectrosc. Relat. Phenom.* **195**, 85 (2014).
- ³¹M. Knupfer, T. Pichler, M. S. Golden, J. Fink, M. Murgia, R. H. Michel, R. Zamboni, and C. Taliani, *Phys. Rev. Lett.* **83**, 1443 (1999).
- ³²R. Schuster, J. Trinckauf, C. Habenicht, M. Knupfer, and B. Büchner, *Phys. Rev. Lett.* **115**, 026404 (2015).
- ³³C. Habenicht, L. Sponza, R. Schuster, M. Knupfer, and B. Büchner, *Phys. Rev. B* **98**, 155204 (2018).
- ³⁴J.-L. Baudour, Y. Delugeard, and P. Rivet, *Acta Crystallogr., Sect. B: Struct. Crystallogr. Cryst. Chem.* **34**, 625 (1978).
- ³⁵B. A. Bolton and P. N. Prasad, *Chem. Phys.* **35**, 331 (1978).
- ³⁶C. Ecolivet, B. Toudic, and M. Sanquer, *J. Phys., Colloq.* **42**, C6-779 (1981).
- ³⁷J. Wasicki, M. Radoska, and R. Radoski, *J. Therm. Anal. Calorim.* **25**, 509 (1982).
- ³⁸K. Saito, T. Atake, and H. Chihara, *J. Chem. Thermodyn.* **17**, 539 (1985).
- ³⁹K. N. Baker, A. V. Fratini, T. Resch, H. C. Knachel, W. W. Adams, E. P. Socci, and B. L. Farmer, *Polymer* **34**, 1571 (1993).
- ⁴⁰K. Zhang and X.-J. Chen, *Spectrochim. Acta, Part A* **213**, 199 (2019).
- ⁴¹K. Zhang, R.-S. Wang, and X.-J. Chen, *Phys. Chem. Chem. Phys.* **21**, 13590 (2019).
- ⁴²Y. Delugeard, J. Desuche, and J. L. Baudour, *Acta Crystallogr., Sect. B: Struct. Crystallogr. Cryst. Chem.* **32**, 702 (1976).
- ⁴³V. A. Postnikov, N. I. Sorokina, O. A. Alekseeva, V. V. Grebenev, M. S. Lyasnikova, O. V. Borshchev, N. M. Surin, E. A. Svidchenko, S. A. Ponomarenko, and A. E. Voloshin, *Crystallogr. Rep.* **63**, 139 (2018).
- ⁴⁴K. Yokouchi, K. Uchida, and Y. Takahashi, *J. Lumin.* **87**, 764 (2000).
- ⁴⁵A. Piaggi, G. Lanzani, G. Bongiovanni, A. Mura, W. Graupner, F. Meghdadi, G. Leising, and M. Nisoli, *Phys. Rev. B* **56**, 10133 (1997).
- ⁴⁶P. Puschnig and C. Ambrosch-Draxl, *Phys. Rev. B* **60**, 7891 (1999).
- ⁴⁷P. Puschnig and C. Ambrosch-Draxl, *Monatsh. Chem.* **139**, 389 (2008).
- ⁴⁸J. Dale, *Acta Chem. Scand.* **11**, 971 (1957).
- ⁴⁹W. J. D. Beenken and H. Lischka, *J. Chem. Phys.* **123**, 144311 (2005).
- ⁵⁰M. Marcus, O. R. Tozer, and W. Barford, *J. Chem. Phys.* **141**, 164102 (2014).
- ⁵¹F. C. Spano, *J. Chem. Phys.* **118**, 981 (2003).
- ⁵²Z. Zhao and F. C. Spano, *J. Chem. Phys.* **122**, 114701 (2005).
- ⁵³W. Kulig and P. Petelenz, *Phys. Rev. B* **79**, 094305 (2009).
- ⁵⁴F. C. Spano, L. Silvestri, P. Spearman, L. Raimondo, and S. Tavazzi, *J. Chem. Phys.* **127**, 184703 (2007).
- ⁵⁵L. Silvestri, S. Tavazzi, P. Spearman, L. Raimondo, and F. C. Spano, *J. Chem. Phys.* **130**, 234701 (2009).
- ⁵⁶P. Chow and B. Friedman, *Phys. Rev. B* **77**, 073406 (2008).
- ⁵⁷A. Gloter, M.-W. Chu, M. Kociak, C. H. Chen, and C. Colliex, *Ultramicroscopy* **109**, 1333 (2009).
- ⁵⁸N. Hiraoka, H. Okamura, H. Ishii, J. Jarrige, K. D. Tsuei, and Y. Q. Cai, *Eur. Phys. J. B* **70**, 157 (2009).
- ⁵⁹A. Sakko, A. Rubio, M. Hakala, and K. Hämäläinen, *J. Chem. Phys.* **133**, 174111 (2010).
- ⁶⁰W. B. Wu, N. Hiraoka, D. J. Huang, S. W. Huang, K. D. Tsuei, M. van Veenendaal, J. van den Brink, Y. Sekio, and T. Kimura, *Phys. Rev. B* **88**, 205129 (2013).
- ⁶¹J. J. Ritsko, N. O. Lipari, P. C. Gibbons, S. E. Schnatterly, J. R. Fields, and R. Devaty, *Phys. Rev. Lett.* **36**, 210 (1976).
- ⁶²M. W. Haverkort, A. Tanaka, L. H. Tjeng, and G. A. Sawatzky, *Phys. Rev. Lett.* **99**, 257401 (2007).
- ⁶³N. Hiraoka, M. Suzuki, K. D. Tsuei, H. Ishii, Y. Q. Cai, M. W. Haverkort, C. C. Lee, and W. Ku, *Europhys. Lett.* **96**, 37007 (2011).
- ⁶⁴T. Willers, F. Strigari, N. Hiraoka, Y. Cai, M. Haverkort, K.-D. Tsuei, Y. Liao, S. Seiro, C. Geibel, F. Steglich *et al.*, *Phys. Rev. Lett.* **109**, 046401 (2012).
- ⁶⁵J. A. Bradley, K. T. Moore, G. van der Laan, J. P. Bradley, and R. A. Gordon, *Phys. Rev. B* **84**, 205105 (2011).
- ⁶⁶K. Yang, L. Chen, Y. Cai, N. Hiraoka, S. Li, J. Zhao, D. Shen, H. Song, H. Tian, L. Bai *et al.*, *Phys. Rev. Lett.* **98**, 036404 (2007).
- ⁶⁷M. Knupfer and J. Fink, *Phys. Rev. B* **60**, 10731 (1999).
- ⁶⁸M. Knupfer, J. Fink, E. Zojer, G. Leising, and D. Fichou, *Chem. Phys. Lett.* **318**, 585 (2000).